Supercond. Sci. Technol. **21** (2008) 045010 (10pp) doi:10.1088/0953-2048/21/4/045010

Quench induced degradation in $Bi_2Sr_2CaCu_2O_{8+x}$ tape conductors at 4.2 K

T Effio[1,2], U P Trociewitz[1], X Wang[1,3] and J Schwartz[1,2,3]

[1] National High Magnetic Field Laboratory, Florida State University, 1800 E. Paul Dirac Drive, Tallahassee, FL 32310, USA
[2] Department of Mechanical Engineering, Florida State University, 2525 Pottsdamer Street, Tallahassee, FL 32310, USA
[3] Department of Electrical Engineering, Florida State University, 2525 Pottsdamer Street, Tallahassee, FL 32310, USA

Received 14 November 2007, in final form 24 January 2008
Published 28 February 2008
Online at stacks.iop.org/SUST/21/045010

Abstract

With the growing interest in commercial Ag-alloy sheathed $Bi_2Sr_2CaCu_2O_{8+x}$ powder-in-tube conductors (Bi2212) for use in high-field magnets, it is important to understand the quench behavior and limiting criteria of a quench, including conditions that will result in a decrease in critical current. Even though the quench characteristics of low-temperature superconductors NbTi and Nb_3Sn are well understood, there is still a lack of data and understanding of what conditions during quenches in high-temperature superconducting (HTS) materials cause degradation of the conductor. In this investigation, quenches are induced in short samples of Bi2212 tape conductors with local heat disturbances using a resistive heater. The voltage and temperature evolution during quenching were recorded and analyzed to determine the normal zone propagation velocity. Furthermore, the quench conditions where varied to identify the threshold quench conditions which result in conductor damage. These conditions are quantified in terms of three parameters: the maximum temperature (T_{max}), the maximum rate of temperature increase ($dT/dt|_{max}$) and the maximum temperature gradient ($dT/dx|_{max}$).

It is found that the normal zone propagation velocity for Bi2212 tape conductor is 20–30 mm s^{-1}. The samples showed high sensitivity during quench, exhibiting large losses in critical current under certain conditions. In all cases the sections of the tape closest to the quench initiation exhibited the highest peak temperatures and loss in critical current. It was found that conductor damage is avoided under the following conditions: $dT/dt|_{max} < 250$ K s^{-1}, $dT/dx|_{max} < 100$ K cm^{-1} and $T_{max} < 250$ K.

1. Introduction

With the growing interest in commercial Ag-alloy sheathed $Bi_2Sr_2CaCu_2O_{8+x}$ powder-in-tube conductors (Bi2212) for use in high-field magnets, it is important to understand the quench behavior and limiting criteria of a quench, including conditions which will result in a decrease in critical current. Even though the quench characteristics of low-temperature superconductors NbTi and Nb_3Sn are well understood, there is still a lack of data and understanding as to which quench conditions in high-temperature superconducting (HTS) materials result in conductor degradation. HTS materials have shown a slower normal zone propagation velocity (NZPV), more localized thermal disturbances, and higher minimum quench energies, and thus quench detection and protection are more difficult [1–5].

In this investigation, quenches were induced in short samples of Bi2212 tape conductors with local heat disturbances using a resistive heater. Preliminary NZPV and minimum quench energies (MQE) were obtained. The voltage and temperature evolution during quenching were recorded and analyzed. The quench conditions were then varied to identify the threshold quench conditions for conductor degradation. While NZPV and MQE may depend on the experiments' characteristics, degradation conditions are likely to be local and thus intrinsic to the conductor. Three quantifiable

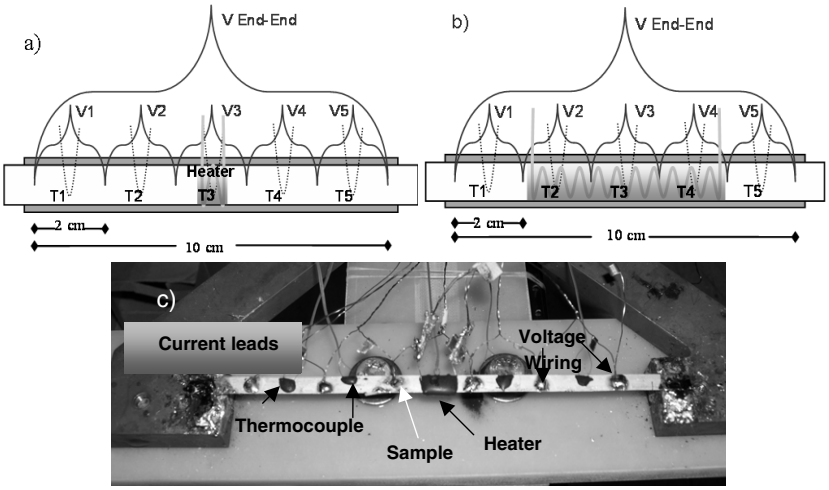

Figure 1. (a) Schematic of the sample mounted with diagnostic wiring for (a) a single-section heater, (b) a three-section heater, and (c) a photograph of sample with a single-section heater. The experimental setup consists of a Bi2212 tape conductor mounted on the probe, which is inserted in liquid helium. A transport current of 350 A is passed through the sample; shortly after, a current of variable amplitude and time is passed through the heater to induce a local 'hot-spot' in the conductor. A quench is induced if the thermal disturbance that is created propagates along the length of the tape through joule heating.

causes of conductor degradation are considered: the maximum temperature ($T_{\max}$), the maximum rate of temperature increase ($\mathrm{d}T/\mathrm{d}t|_{\max}$) and the maximum temperature gradient ($\mathrm{d}T/\mathrm{d}x|_{\max}$). During a disturbance, whether it is a stable recovery or a quench T, $\mathrm{d}T/\mathrm{d}x$ and $\mathrm{d}T/\mathrm{d}t$ are both spatially and temporally varying. Thus, here the maximum values refer to both spatial and temporal maxima. The method for determining the maximum values is described later in the paper.

2. Experimental approach

The experimental approach involved mounting Bi2212 tape conductor samples on a quench probe with an attached heater and both voltage and temperature measurement instrumentation, introducing a steady-state transport current, and pulsing the heater. The conductor temperatures and voltages are then monitored as a function of time to determine if a quench ensues. If not then, after equilibrium is reestablished, the experiment is repeated with the pulse amplitude increased. This section describes the experimental approach in greater detail, as do previous reports on other HTS conductors [1, 2].

2.1. HTS conductor samples

Commercial 19-filament Bi2212 tape conductor was obtained from Oxford Superconducting Technology. The Bi2212 tape cross-section was 0.22 mm × 5.00 mm. The end-to-end self-field critical current (I_c) at 4.2 K was 450 A, determined using a 1 μV cm^{-1} electrical field criterion with a 10 cm voltage tap separation on a 12 cm length of conductor. This corresponds to a self-field engineering critical current density (J_e) at 4.2 K of 409 A mm^{-2}. The average n-value at 4.2 K, self-field was 12. The same conductor was used previously in the high-field insert coil reported in [6] and in the statistical study of electromechanical properties [7]. Conductor parameters are presented in table 1.

Table 1. Summary of conductor parameters.

Parameter	Value
Filament count	19
Cross-section	0.22 mm × 5.00 mm
Average n-value	12
Average critical current	450 A
Average J_e	409 A mm^{-2}

2.2. Heater

A silicon-insulated nickel–chromium alloy heater wire is bent in the form of a 'W' and mounted on the surface of the Bi2212 tape using cyanoacrylate glue. The heater is then covered by aluminum-filled black epoxy and cured for 24 h at room temperature. The nickel–chromium alloy has a resistivity of 0.661 Ω cm^{-1} at 20 °C [1, 2]. Two lengths of heaters are used in these experiments and are referred to as 'single-section heater' and 'three-section heater', as described below. The single-section heater has a measured resistance of $R_{\text{heater}} \sim 3\ \Omega$.

2.3. Experimental configuration

The Bi2212 tape is mounted onto the copper current leads of a quench probe. Figure 1 shows the experimental setup, including the sample, heater, instrumentation wiring (voltage and thermocouple), and copper current leads. The heater is mounted in the middle of the sample and five voltage taps are distributed evenly across 10 cm of the sample. This creates five 'sections' of the tape on which the voltage as a function of time can be monitored during a quench, and a sixth section which covers the full 10 cm. The voltage taps are soldered onto

the sample using Sn60/Pb40 solder. E-type thermocouples are placed in the center of each section and monitored throughout the experiment. Finally, the sample is reinforced with a 12 cm piece of G-10, adhered to the back of the sample with a thin layer of alumina-filled epoxy. The thermocouple junctions are placed between the sample and the G-10 strip. Lastly, two pairs of copper wires are soldered to the heater; one pair serves as current leads to the heater, and the other for monitoring $V_{\text{heater}}(t)$.

To vary the initial hot-spot size and gain more insight into the quench behavior and degradation conditions, two heater geometries are used in parallel experiments. In the first version, the heater length is within the center section of the conductor. In the second version, a longer heater is used such that it covers sections 2–4 (where section 3 is the center section of the conductor). By expanding the initial hot-spot length, the temperature distribution is varied in a controlled manner. Using a larger heater, the temperature differences between the three sections can be reduced, depending on the amplitude and duration of the heater voltage pulse. This allows for the creation of a variety of quench situations, varying the time for the conductor to begin thermal runaway, and the time for the quench to evolve.

The transport current through the sample was measured across a precision shunt of 100 mV/1000 A. Voltage taps $V_{\text{End–End}}$, V1 and V2 were connected to digital multimeters (DMM). The readings from voltage taps V3, V4 and V5 were recorded by a fast-speed digital storage oscilloscope. The thermocouple wires were connected to another set of DMMs. The voltage drop across the heater was recorded using the digital oscilloscope in parallel with an additional DMM. The voltmeters and the oscilloscope were connected to a computer via a GPIB for simultaneous readout. To increase the data acquisition speed, some voltmeters were set to burst mode, writing first to the internal buffer communicating with the computer. The entire experiment was controlled via GPIB using LabVIEW software. More details of the monitoring are described in [1].

2.4. Experimental method

After attaching the instrumentation described previously, the sample is cooled in liquid helium (LHe) and the sample critical current is measured for each section using a 1 μV cm^{-1} electrical field criterion. For this conductor, the end-to-end self-field $I_c \sim 450$ A. A transport current of 350 A is then initiated in the conductor ($\sim$78%I_c). A thermal disturbance is then introduced by pulsing a current into the heater with a pulse generator connected to a fast four-quadrant power supply. Both the pulse duration and amplitude can be varied. $V(t)$ and $T(t)$ for each section are recorded for the duration of the experiment. A quench is determined to have occurred if the $V(t)$ and $T(t)$ responses indicate a thermal runaway. The transport current is shut off when the voltage reading over the entire 10 cm reaches some specified value, typically 0.3 V. Note that the voltage limit directly affects $T_{\max}$.

If instead of a quench there is recovery, then the conductor is considered stable and the experiment is repeated with the pulse amplitude increased in small steps (0.05 V) until a quench occurs. Note that the pulse duration is held constant for most experiments (300 ms). The minimum heater pulse resulting in a quench is then the minimum quench energy. This approach is the same as reported previously on other HTS conductors [1, 2, 8, 9].

In the case of a quench, the normal zone propagates in both directions from the center section due to the continued joule heating effect caused by current sharing of the transport current. The normal zone propagation velocity (NZPV) is determined by the time lag for a fixed voltage to be measured from one section to the next; again, this approach has been reported previously [1].

The I_c of each section is re-measured after each heater pulse, whether it resulted in recovery or a quench. In this way, the effects of quenching on conductor performance are determined.

The procedure for the three-section heater experiments is primarily the same as the one-section experiments, but two extremes are investigated. In one set of experiments, the heater voltage is large and over a short period of time; in the second, the heater voltage is small but for a longer duration. The first scenario is intended to create a relatively uniform temperature distribution in the three middle sections with high $\mathrm{d}T/\mathrm{d}t$. The second scenario is intended to result in a small $\mathrm{d}T/\mathrm{d}t$ and $\mathrm{d}T/\mathrm{d}x|_{\max} < 100$ K cm^{-1}. With a long heater pulse it is expected that sections 2–4 will have a less homogeneous temperature distribution than with a short heater pulse. This is due to greater heat removal from the outer heater sections than the middle section. The heat removal is not as visible in the previous experiments because of the high power input into the heater and the short heater pulse. However, temperature rises in all three heater sections are expected, creating a relatively low $\mathrm{d}T/\mathrm{d}x$ in the conductor, even without a homogeneous temperature distribution.

2.5. Data analysis

The MQE is determined as the minimum heater energy required to induce a quench. The heater energy (E_{heater}) is determined using

$$E_{\text{heater}} = \frac{V_{\text{heater}}^2}{R} t \tag{1}$$

where V_{heater} is the voltage across the heater, R is the heater resistance and t is the pulse duration.

The energy dissipated in each section of the conductor due to joule heating (E) is calculated using

$$E = \int_0^{t_{\text{end}}} V(t) I \, \mathrm{d}t \tag{2}$$

where t_{end} is the time at which the experiment is ended, $V(t)$ is the measured voltage in a section as a function of time and I is the transport current. In applying this equation, the effect of current sharing is neglected and $I = 350$ A is used. Thus, it is assumed that during a quench, the time for which the current sharing temperature $T_{cs} < T < T_c$ is short and the entire transport current is in the Ag-alloy sheath. The temperature

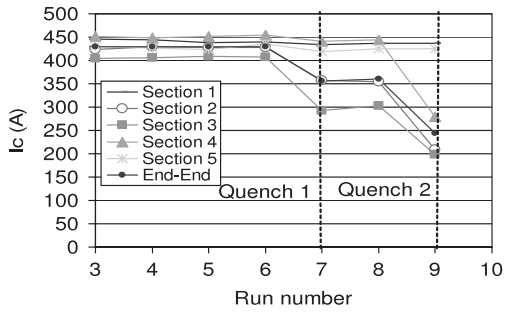

Figure 2. Typical I_c versus run number for each section of a sample. A run is considered an attempt to induce a quench via a heat pulse. The heater input energy is increased from run to run, until the first quench results in Run 7. There is no loss in I_c following runs where no quench occurred. I_c is reduced after each quench. The goal is to identify the quench conditions that cause a loss in I_c so that quench detection and protection schemes can be developed to avoid such conditions.

dependence of I_c in Bi2212 is strong, so this is a reasonable approximation.

To understand the physical meaning of $\mathrm{d}T/\mathrm{d}x|_{\max}$, $\mathrm{d}T/\mathrm{d}t|_{\max}$ and E, it is important to define the convention by which these parameters were obtained and how experimental variations may affect them. $\mathrm{d}T/\mathrm{d}x$ is calculated by taking the temperature difference from one section to the adjacent section as a function of time. The maximum value of $\mathrm{d}T/\mathrm{d}x(x,t)$ can be calculated as a function of section and time; the maximum value is reported as $\mathrm{d}T/\mathrm{d}x|_{\max}$. Similarly, $\mathrm{d}T/\mathrm{d}t(t)$ is calculated for each section (x-location) by taking the difference in temperature from one time-step to the next, and dividing that temperature difference by the time between the said data points. This procedure is performed for each section, and the maximum value of $\mathrm{d}T/\mathrm{d}t(x,t)$ is reported as $\mathrm{d}T/\mathrm{d}t|_{\max}$. The time difference between data points is defined by the DMMs buffer speed, and is 0.04 s. $\mathrm{d}T/\mathrm{d}t(x,t)$ is calculated from the time at which the heat pulse is initiated until t_{end}.

It is important to recognize that t_{end} is determined by the voltage criterion used to end the experimental run; it is not an intrinsic property of the conductor. Varying t_{end} affects $T_{\max}$ and E (through equation (2)) and thus provides a method for varying $T_{\max}$ without necessarily changing $\mathrm{d}T/\mathrm{d}x|_{\max}$ or $\mathrm{d}T/\mathrm{d}t|_{\max}$. Thus, changing t_{end} is a method for manipulating the quench characteristics in the conductor so as to distinguish which parameters most affect degradation.

3. Results

3.1. Single-section heater experiments

While the typical sample I_c is 450 A, it is important to note that the samples are inhomogeneous along the length. These variations, which are about ±7% initially, are seen in figure 2, which shows the I_c of each section as a function of run number (a run is considered to be an attempt to induce a quench in the sample, i.e. a heater pulse). I_c varies from 410 to 460 A, with end-to-end $I_c = 430$ A. Runs 1–6 did not have sufficient heater energy to induce a quench. After Run 7 (Quench 1) and Run 8 (Quench 2) there is a considerable drop in I_c in sections 2–4. The heater energy in Quench 1, 3.82 J, is only 6% more than that of Run 6. In the runs before Quench 1, there is no loss of I_c in any conductor section. Thus conductor degradation (loss of I_c) is introduced in the sample only due to quenching.

Typical $V(t)$ plots during a quench are shown in figure 3(a). In this case, the applied heater energy of 3.82 J equals the minimum quench energy (MQE) under these conditions ($I_t = 350$ A, $I_c = 450$ A, $T = 4.2$ K). It is important to note that, while section three of the tape exhibits a large increase in voltage during a quench, the sections furthest away from the heater (1 and 5) exhibit little or no voltage rise. This illustrates the slow normal zone propagation in this conductor. Using the method described in [1, 2], the NZPV is 20–30 mm s^{-1}. Note that, in general, the heater setup can result in some sample-to-sample variation because of differences in, for example, the amount of Stycast used to adhere the heater to the conductor surface and the amount of wire used to form the heater, causing the MQE to vary from 3 to 5 J, deposited over a surface area of 50 mm^2 (volume of ∼11 mm^3). The $T(t)$ data in sections 1–5 (corresponding to the $V(t)$ data in figure 3(a)) is shown in figure 3(b). The center section (section 3) experiences $T_{\max} > 240$ K, while the temperatures in sections 1 and 5 rise by ∼10 K.

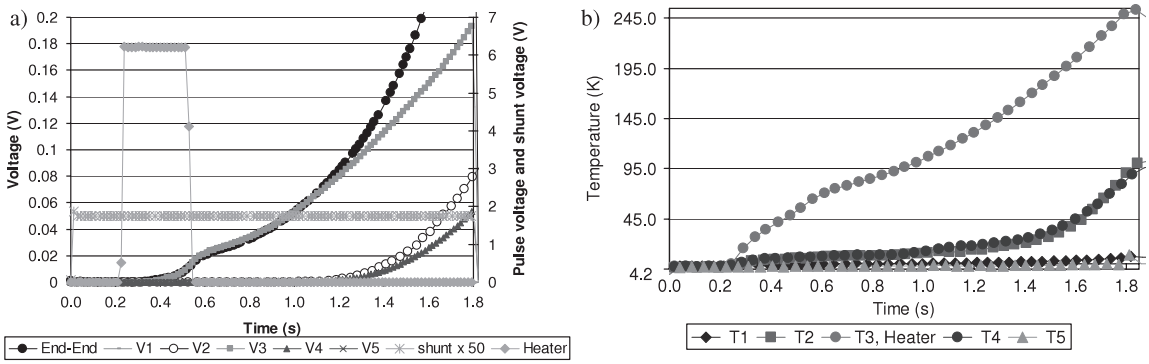

Figure 3. $V(t,\text{section})$ and $T(t,\text{section})$ data collected from a single-section-heater quench experiment. (a) Typical voltage traces at the minimum quench energy (3.82 J) section 3 exhibits large increases in voltage, while sections 1 and 5 exhibit little or no voltage rise. (b) Corresponding $T(t)$; section 3 has large temperature increases, while sections 1 and 5 only have temperature rises of about 10 K. (a) and (b) correspond to Quench 1 in figure 4.

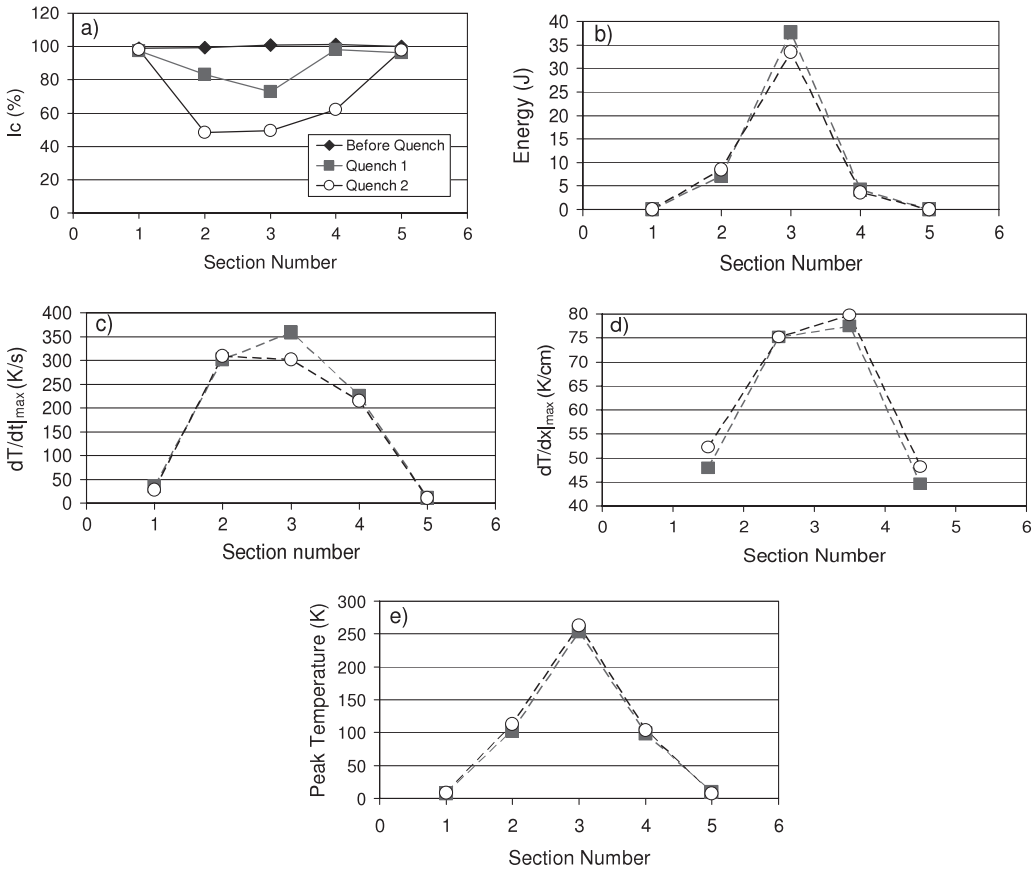

Figure 4. Results for a single-section heater experiment. (a) I_c normalized to the as-processed I_c versus location along the length of the tape (section number); (b) energy dissipated into the tape versus section number; (c) $dT/dt|_{max}$ versus section number; (d) $dT/dx|_{max}$ versus section number; (e) peak temperature versus section number. Conductor degradation is observed after Quench 1 (25% reduction in I_c in section 3). Further degradation is seen after Quench 2 under similar quench conditions. It is important to note that a $dT/dt|_{max}$ of 303 K s^{-1} and a $dT/dx|_{max} < 80$ K cm^{-1} cause this relatively large loss in I_c. Trying to manipulate these conditions may result in a non-damaging quench.

This localization of the temperature rise during a quench is consistent with the $V(t)$ data shown in figure 3(a).

Figures 4(a) and (b) shows the energy dissipated in each section of the conductor during a quench, along with the normalized critical current before and after quenching. This is the energy from the continued joule heating, and is calculated via numerical integration using equation (1). The energy during quench is localized, and the most damage occurs in the heater section. Figures 4(c)–(e) shows $dT/dt|_{max}(x)$, $dT/dx|_{max}(x)$ and $T_{max}(x)$, which are determined using the T(section, t) data during a quench.

3.2. Three-section heater experiments

As described in section 3.1 above, the temperature profile in the single-section heater experiments is highly peaked and thus it may be difficult to distinguish between the effects of $dT/dx|_{max}(x)$ and $T_{max}(x)$. This may be an important distinction for Bi2212, because the superconductor itself is brittle and contains a variety of pre-existing defects, such as second phases and porosity, which are known to affect the electromechanical performance [10]. In order to have some independent control of $dT/dx|_{max}(x)$ and $T_{max}(x)$, three-section heater experiments were performed.

Figure 5 shows the $V(t)$ and $T(t)$ data of a quench experiment in which $dT/dx|_{max}(x) < 25$ K cm^{-1} in the three middle sections. The heater energy was 1 J with a 150 ms pulse (6.7 J s^{-1}). In figure 5(a) it is seen that the quench occurs in all three sections simultaneously with a comparable voltage rise. The spatially uniform rise in temperature over the three middle sections mirrors the $V(t)$ behavior.

Figures 6(a)–(e) illustrates the quench conditions in terms of energy from joule heating, $dT/dt|_{max}(x)$, $dT/dx|_{max}(x)$ and $T_{max}(x)$, along with the normalized critical current. As with the single-section heater experiments, degradation occurred only when a quench was induced, and it was also not possible to induce a quench without degrading the conductor. Although the energy dissipated into the conductor is smaller than in the single-section heater experiment (only 15 J in section 3 of Quench 1), this is due to the short quench time ($t_{end} = 0.8$ s). dT/dt is rapid in these quenches; $dT/dt|_{max}$ (section 3) ~460 K s^{-1} during Quench 1, which is ~30% higher that the single-section heater result. T_{max} and $dT/dx|_{max}$ in section 3 during Quench 1 remained low: 200 K and 25 K cm^{-1}, respectively. There is a loss of 18% I_c in section 3 during Quench 1, while in the single-section heater experiments there was a loss of 25% I_c. Section 2 during Quench 1 experienced

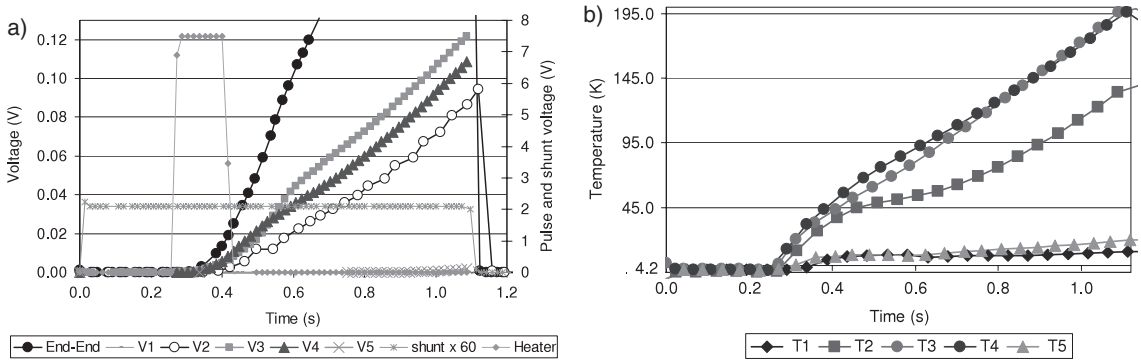

Figure 5. Voltage and temperature evolution of a three-section heater quench experiment, in which the temperature over the three middle sections is relatively uniform (energy applied to heater 1 J over 150 ms). This experiment is conducted to reduce $\mathrm{d}T/\mathrm{d}x|_{\max}$ while keeping $\mathrm{d}T/\mathrm{d}t|_{\max}$ large in order to delineate their respective effects on I_c loss. (a) $V(t)$; (b) $T(t)$. Voltages in sections 2–4 rise together, as well as the temperatures in sections 2 and 3. (a) and (b) correspond to Quench 1 in figure 6.

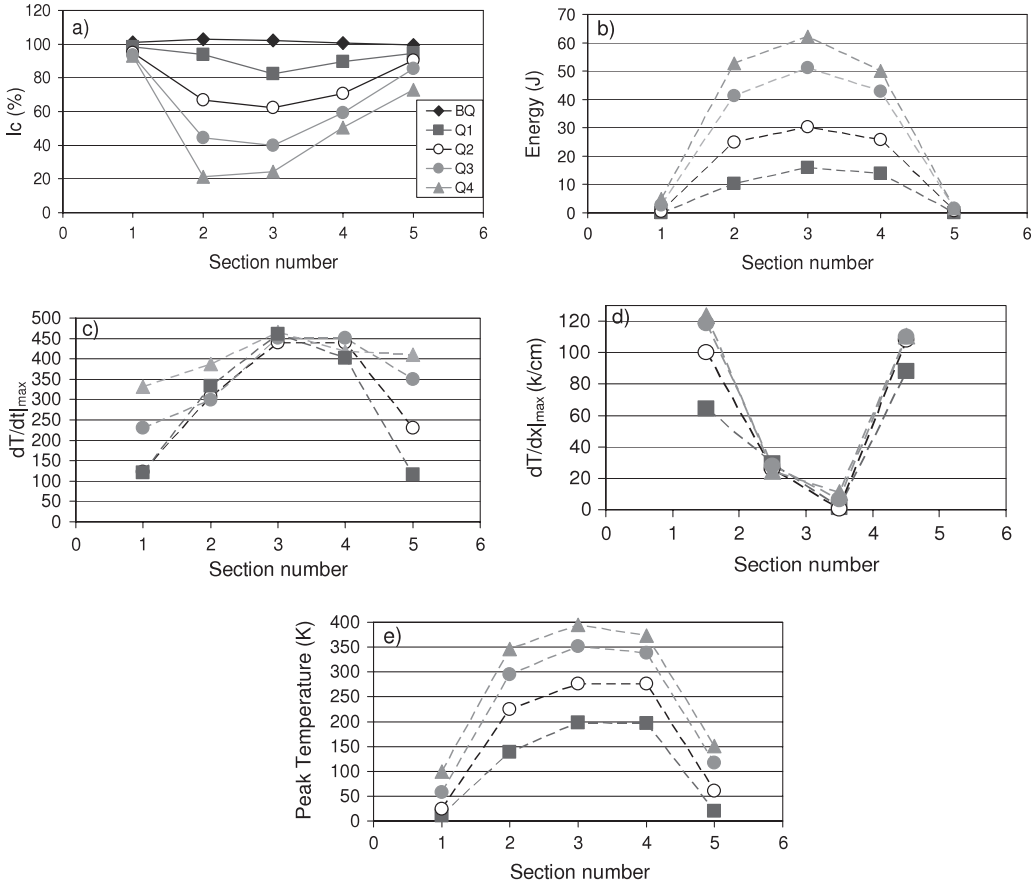

Figure 6. Data analysis results from a three-section-heater experiment in which $\mathrm{d}T/\mathrm{d}x_{\max}$ is kept small, but $\mathrm{d}T/\mathrm{d}t|_{\max}$ is large. (a) I_c normalized to the as-processed I_c versus section number; (b) energy dissipated into the tape versus location; (c) $\mathrm{d}T/\mathrm{d}t|_{\max}$ versus section number; (d) $\mathrm{d}T/\mathrm{d}x|_{\max}$ versus section number; (e) peak temperature versus section number. $\mathrm{d}T/\mathrm{d}x$ over section 3 is kept small in all quenches, with large $\mathrm{d}T/\mathrm{d}t$ and $T_{\max}$. Damage is evident in all quenches: Before Quench (BQ), Quench 1 (Q1), Quench 2 (Q2), Quench 3 (Q3), Quench 4 (Q4). It is evident that simply reducing $\mathrm{d}T/\mathrm{d}x|_{\max}$ is not sufficient in neutralizing the damaging effects of a quench.

a loss of 7% I_c, along with a small $T_{\max}$, but $\mathrm{d}T/\mathrm{d}t|_{\max} \sim 333\ \mathrm{K\ s^{-1}}$ and $\mathrm{d}T/\mathrm{d}x|_{\max} \sim 60\ \mathrm{K\ cm^{-1}}$.

Figure 7 shows the $V(t)$ and $T(t)$ data of a quench experiment where the heater pulse amplitude is lower but the pulse duration is longer, >900 ms, resulting in a heater energy of 5 J (5.5 J s^{-1}). This creates a less uniform temperature distribution and a smaller $\mathrm{d}T/\mathrm{d}t$ over sections 2–4 than in the previous experiment.

Figure 8 shows the quench conditions in terms of $E(x)$, $\mathrm{d}T/\mathrm{d}t|_{\max}(x)$, $\mathrm{d}T/\mathrm{d}x|_{\max}(x)$ and $T_{\max}(x)$, along with the normalized critical current. The energy dissipated in section 3 during Quench 1 was large, 33 J, but this occurs over 1.9 s

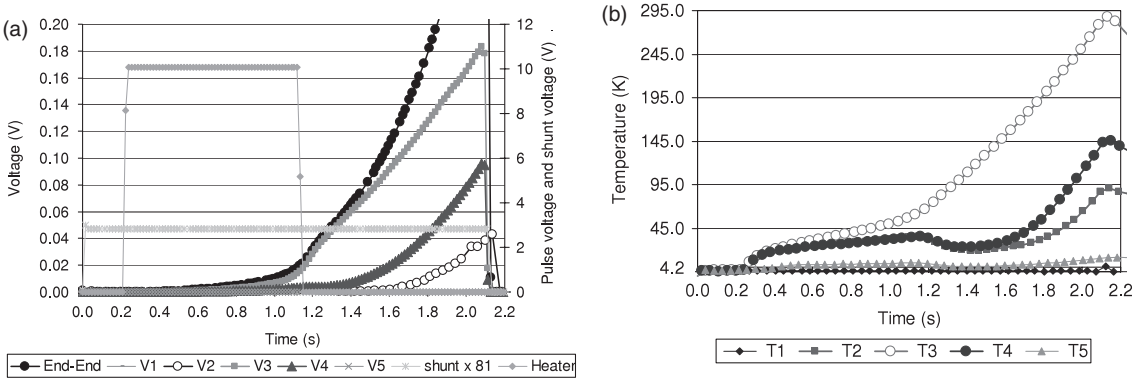

Figure 7. Voltage and temperature evolution of a three-section heater quench experiment where $\mathrm{d}T/\mathrm{d}t|_{\max}$ is kept small, with moderate $\mathrm{d}T/\mathrm{d}x|_{\max}$ and $T_{\max}$. These thermal behaviors are achieved by applying a small-amplitude current to the heater over 900 ms, allowing for a slow rise in temperature over the heater sections. $T_{\max}$ is kept moderate by regulating t_{end}, the time at which the transport current is shut off, effectively ending the experiment and removing the joule heating that drives the temperature rise. (a) $V(t)$ and (b) $T(t)$, corresponding to Quench 1 in figure 8.

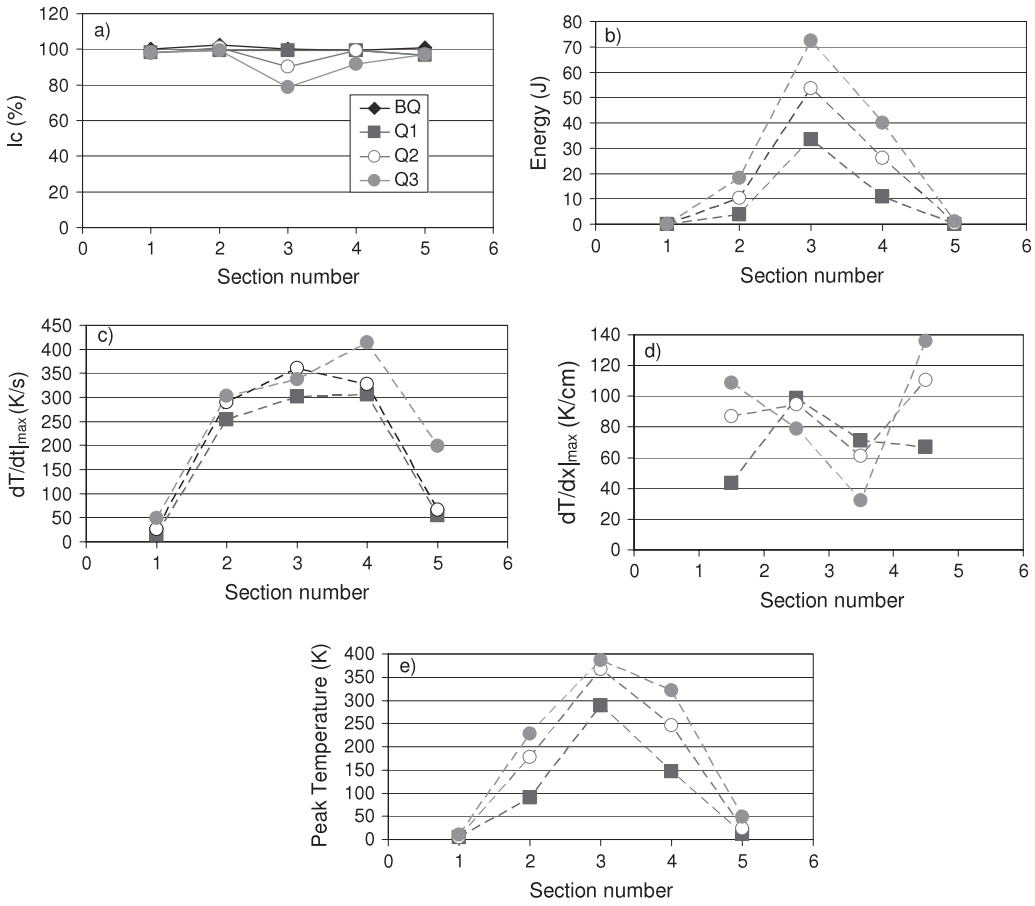

Figure 8. Data analysis results from a three-section-heater quench experiment where $\mathrm{d}T/\mathrm{d}t|_{\max}$ is kept small and $\mathrm{d}T/\mathrm{d}x|_{\max} T_{\max}$ are kept at moderate values. (a) I_{c} normalized to the as-processed I_{c} versus section number; (b) energy dissipated into the tape versus location; (c) $\mathrm{d}T/\mathrm{d}t|_{\max}$ versus section number; (d) $\mathrm{d}T/\mathrm{d}x|_{\max}$ versus section number; (e) peak temperature versus section number. $\mathrm{d}T/\mathrm{d}t$ is kept low, with moderate $\mathrm{d}T/\mathrm{d}x$ and moderate $T_{\max}$. There is no damage from Quench 1, and thus threshold quench conditions that do not incur a loss of I_{c} can be determined.

(17.4 J s^{-1}), which is a much longer time than in previous quenches. $\mathrm{d}T/\mathrm{d}t$ is low, with $\mathrm{d}T/\mathrm{d}t|_{\max} \sim 300$ K s^{-1} during Quench 1 in section 3. $\mathrm{d}T/\mathrm{d}x$ was also low, with $\mathrm{d}T/\mathrm{d}x|_{\max} < 100$ K cm^{-1} during Quench 1, and typically <80 K cm^{-1}. $T_{\max}$ approached 300 K. As seen in figure 8(a), these conditions did not cause a loss in I_{c} during Quench 1. Figure 8(a) also shows that damage was first induced in the conductor during Quench 2, where the quench conditions

Table 2. Summary of quench conditions and resulting loss in I_c: Quench 1 figure 4. Quenching was induced using a heater over section 3 and allowing the transport current to propagate the induced normal zone. $V(t)$ and $T(t)$ data were then analyzed to determine resulting quench conditions. $dT/dx|_{max}$ is reported as the maximum temperature gradient between sections, and its values are inserted between section columns. It is important to note the extreme localization of energy and temperature in section 3 of the quench, resulting in large loss in I_c over the section.

	Sec.1		Sec.2		Sec.3		Sec.4		Sec.5
Energy/time (J s^{-1})	0.0		4.7		25.1		2.8		0.0
$dT/dt|_{max}$ (K s^{-1})	34.5		302.9		357.9		224.0		10
$dT/dx|_{max}$ (K cm^{-1})		47.9		75.2		77.5		44.6	
T_{max} (K)	7.0		102.8		253.2		98.3		9.1
Loss I_c (%)	**2.5**		**17.0**		**27.3**		**1.9**		**3.6**

were more extreme, leading to $dT/dt|_{max} > 350$ K s^{-1} and $T_{max} > 350$ K.

4. Discussion

The severity of a quench in LHe at self-field is reflected through figure 2. A loss in critical current is observed only after quenching, but not during runs where the heat pulse did not cause thermal runaway. A difference in heater energy of only 0.25 J in a volume of ∼11 mm^3 is the measured difference between a quench that results in degradation and a recoverable thermal disturbance. The $V(t)$ and $T(t)$ data in figure 3 show that there are significant temperature and voltage rises in the central section (section 3) of the tape but, even as the central section reaches temperatures above 240 K, there is only minimal temperature increase in sections 1 and 5. Thus the timescale for conductor degradation is much shorter than propagation. While a hot-spot may experience a large temperature increase during a quench, a location less than 5 cm away may have no change. The combination of finite MQE and slow NZPV places a heavy burden on potential magnet protection systems using such a conductor. The protection system must be sufficiently sensitive to distinguish between a quench and thermal disturbance and fast enough to protect the magnet.

From figure 4, which illustrates the single-section heater results, threshold values for the thermal conditions that degrade the conductor are difficult to determine. It is clear, however, that relatively small values for dT/dt are required to keep the conductor safe; i.e. the conductor is sensitive to thermal shock. In this particular example, a $dT/dt|_{max}$ of 358 K s^{-1} results in a reduction of 27% I_c. Coupled to that is the relatively low $T_{max} \sim 250$ K, despite the relatively large reduction in I_c. Also seen in figure 4(d) is that the temperature increase is localized to the section of the conductor under the heater. There is a difference in temperature from the heater section to the adjacent sections of nearly 160 K. These values are summarized in table 2. To determine which parameters dominate degradation and to determine the safe operating ranges, it is essential that the quench is less localized, both in terms of energy dissipation and temperature homogeneity.

An interesting observation that can be made from figures 3 and 4 is that sections 2 and 4 are exposed to similar quench conditions during Quench 1. Section 2, however, experiences a loss of 17% of I_c, while section 4 only loses 2%. $T(t)$ data from figure 3 is comparable for both sections; $V(t)$ data shows a faster dV/dt in section 2, and thus 3 J more is dissipated into section 2 than into section 4. Sections 2 and 4 initially have critical currents of 428 and 454 A, respectively. It is expected that, as I gets closer to I_c, current sharing between the superconductor and the Ag sheath will occur with smaller heat disturbances [1, 2]. Thus, section 2 responds to the normal zone before section 4, causing a measurable voltage rise at a lower temperature; i.e. the section with the lower initial I_c also has a lower T_{cs}. This phenomenon is reflected in the difference between $dT/dt|_{max}$ values; section 2 has a $dT/dt|_{max}$ of 80 K s^{-1} larger than section 4. Furthermore, it has recently been shown that the electromechanical behavior of Bi2212 tapes is inhomogeneous, so the electromechanical response (i.e. conductor degradation) to comparable thermal conditions is also likely to be inhomogeneous [7]. It is difficult to predict how sections with varying I_c will behave during a quench; however, it is visible that a minimal difference in energy dissipation and $dT/dt|_{max}$, which is in part driven by inhomogeneous I_c distributions, can result in severe disparity in I_c degradation.

A large heat pulse amplitude for a short duration in a three-section heater quench created a relatively low $dT/dx|_{max}$ and a relatively large $dT/dt|_{max}$. This is seen in figure 5. Table 3 summarizes the conditions and the extent of degradation in the conductor. Comparing the data in tables 2 and 3, it is evident that the degradation is not as severe as in the single-heater experiments. Section 2 during Quench 1 has a low T_{max} and moderate $dT/dt|_{max}$ and $dT/dx|_{max}$, and experiences a loss of only 6% of I_c. From this it can be said that, while all three thermal characteristics of a quench can be correlated with conductor degradation, if at least two are limited to moderate values then the degradation is also reduced.

In figures 6(a)–(e), which plots the results from a series of quenches in a three-section heater experiment, it is seen that section 2 has the greatest net reduction in I_c after Quench 4. Section 2 is not, however, the section with the highest T_{max} or $dT/dt|_{max}$, but it is the section with the highest $dT/dx|_{max}$. This is likely to be due to the variations in electromechanical behavior in the conductor, as described in [7]. It is also evident that both dT/dt and dT/dx influence quench induced conductor degradation.

The second three-section-heater scenario, in which $dT/dt|_{max}$ is low and $dT/dx|_{max}$ is moderate, shows promising results. This is the only situation in which it was possible to induce a quench in the tape without causing a reduction in I_c, as shown in figure 8(a). The quench conditions shown

Table 3. Summary of quench conditions and resulting loss in I_c: Quench 1 figure 6. Quench was induced using a three-section-heater over sections 2–4 of the conductor. A large amplitude current pulse over a short time fed to the heater allows for quench conditions in which $dT/dx|_{max}$ is kept at small values over the middle three sections, but $dT/dt|_{max}$ is large. Loss of I_c is still evident in all sections of the conductor, leading to the conclusion that $dT/dx|_{max}$ is not the sole contributor to conductor degradation.

	Sec.1		Sec.2		Sec.3		Sec.4		Sec.5
Energy/time (J s^{-1})	0.0		12.4		19.5		17.0		0.0
$dT/dt|_{max}$ (K s^{-1})	121.2		333.5		460.8		401.2		115.7
$dT/dx|_{max}$ (K cm^{-1})		64.0		29.6		1.3		88.0	
T_{max} (K)	11.3		139.3		198.5		196.0		20.0
Loss I_c (%)	**1.6**		**6.2**		**17.6**		**10.3**		**5.6**

Table 4. Summary of quench conditions and resulting loss in I_c: Quench 1 figure 8. Quench was induced using a three-section heater over sections 2–4 of the conductor. A small amplitude current over 900 ms is used to create a quench condition in which $dT/dt|_{max} < 300$ K s^{-1} and $dT/dx|_{max} < 100$ K cm^{-1}. In this case, no loss in I_c is incurred due to the quench, and threshold values for quench conditions that will not degrade the conductor can be determined.

	Sec.1		Sec.2		Sec.3		Sec.4		Sec.5
Energy/time (J s^{-1})	0.0		1.9		17.6		5.7		0.0
$dT/dt|_{max}$ (K s^{-1})	14.9		254.1		301.8		306.3		54.9
$dT/dx|_{max}$ (K cm^{-1})		43.4		98.7		71.2		67.2	
T_{max} (K)	4.2		91.0		288.3		146.0		11.6
Loss I_c (%)	**1.6**		**0.5**		**0.6**		**0.6**		**1.4**

in figures 8(b)–(e) show that the tape did not degrade if $dT/dt|_{max} < 300$ K s^{-1}, $dT/dx|_{max} < 100$ K cm^{-1}, and $T_{max} < 300$ K. These quench conditions are summarized in table 4. However, from table 2 it is evident that $T_{max} = 250$ K and $dT/dt|_{max} = 303$ K s^{-1} correlates to I_c reductions of 27% and 17%, respectively. Quench conditions similar to these were observed during the single-section-heater experiments, as noted in table 2. The stark dissimilarity between this three-section-heater quench and the above single-section-heater quench is the duration of the heat pulse and accordingly, the time over which the quench was initiated and the energy dissipated into the conductor. From the single-heater-section experiments, 37 J was dissipated over 1.5 s, with a power applied to the heater of 12.75 J s^{-1} over 300 ms. This three-section-heater experiment experienced 33 J dissipated over 1.9 s and a heater power of 5.5 J s^{-1} over 900 ms. It is important to note that the energy applied to the heater in these quench scenarios is never more than 10% of the energy dissipated into the conductor from joule heating over the heater section. It can then be said that, while the heater energy is critical to initiating the quenches, the thermal spike associated with the heat pulse alone does not cause conductor degradation.

Although table 2 shows a reduction in I_c correlating to $dT/dt|_{max} = 303$ K s^{-1} in section 2, this can result from crack propagation due to $dT/dt|_{max} = 357$ K s^{-1} in section 3. In the quench summarized in figure 8, two of the three thermal behaviors remained at moderate values, with $dT/dt|_{max} \sim 300$ K s^{-1} and $dT/dx|_{max} \sim 100$ K cm^{-1}. For all experiments, I_c reduction is avoided if $dT/dt|_{max} < 250$ K s^{-1}. These values are such that severe conductor degradation does not result. An interesting observation is the effect of the energy dissipation on the I_c reduction. While it is expected that increased energy dissipated per cross-sectional area is more damaging, the energy dissipation per time (i.e. power) also contributed. It would be expected that the power per section is reflected in the temperature evolution, especially in terms of T_{max} and $dT/dt|_{max}$. As seen by comparing the single-section-heater experiments to the three-section heater experiments, however, lower power dissipation may not always cause lower T_{max}. Thus, the time required for a quench to develop is also important.

5. Conclusion

An experimental methodology has been developed to initiate normal zone propagation in Bi2212 tape while varying the temperature profile. Multiple voltage taps and thermocouples, monitored by digital multimeters, measured the sample voltage and temperature as a function of time and location.

The results of normal zone propagation velocity and minimum quench energy measurements have been presented. In liquid helium, for this experimental setup, the NZPV is about 20 mm s^{-1}. The minimum quench energy ranges from 3 to 5 J, depending on the specific heater setup, the amount of epoxy used and the critical current of the conductor. It is necessary to calibrate the heater and more accurately determine the amount of energy deposited into the HTS conductor to obtain a clearer conclusion.

Although MQE and NZPV are characteristic of this experimental design, intrinsic conductor information can be obtained by analyzing the affects of the quench thermal behavior on the electrical performance of the conductor. From $T(t)$ data, there are three quantifiable parameters that correlate to conductor damage: T_{max}, $dT/dx|_{max}$ and $dT/dt|_{max}$. While it was not possible to induce a non-damaging quench in the single-section-heater experiments, and thus not possible to determine precisely the threshold values for damage, the three-section-heater experiments succeeded in varying these conditions during a quench to determine their acceptable ranges. It was discovered that maintaining moderate values for $dT/dx|_{max}$ and $dT/dt|_{max}$ effectively reduces conductor

degradation. Furthermore, the amount of energy dissipated via joule heating is important for determining the potential damage of a quench. For this particular Bi2212 tape, it was determined that a $\mathrm{d}T/\mathrm{d}t|_{\max} < 250\ \mathrm{K\ s^{-1}}$, a $\mathrm{d}T/\mathrm{d}x|_{\max} < 100\ \mathrm{K\ cm^{-1}}$ and an energy dissipation of 33 J over 1.9 s are acceptable conditions for avoiding degradation. These are fairly moderate values in comparison to other quench experiments on other conductors, and it reflects the sensitivity of this conductor to a quench under these conditions. Essentially, a quench must be small in intensity and developed over a large area to prevent conductor degradation.

Acknowledgments

The authors would like to thank Oxford Superconducting Technology for providing Bi2212 tape samples for experimentation. The authors also thank Honghai Song, Tengming Shen and Xiaotao Liu for their continued assistance and heat treatment of samples for experimentation.

References

[1] Wang X, Trociewitz U P and Schwartz J 2007 Near-adiabatic quench experiments on short YBa2Cu3O7-δ coated conductors *J. Appl. Phys.* **101** 053904

[2] Trillaud F, Palanki H, Trociewitz U P, Thompson S H, Weijers H W and Schwartz J 2003 Normal zone propagation experiments on HTS composite conductors *Cryogenics* **43** 271–9

[3] Laquer H L, Edeskuty F J, Hassenzahl W V and Wipf S L 1989 Stability projections for high temperature superconductors *IEEE Trans. Magn.* **25** 1516–9

[4] Grabovickic R, Lue J W, Gouge M J, Demko J A and Duckworth R C 2003 Measurements of temperature dependence of the stability and quench propagation of a 20 cm long RABiTS Y–Ba–Cu–O tape *IEEE Trans. Appl. Supercond.* **13** 1726–30

[5] Romanovskii V R and Watanabe K 2006 Operating modes of high-Tc composite superconductors and thermal runaway conditions under current charging *Supercond. Sci. Technol.* **19** 541–50

[6] Weijers H, Trociewitz U P, Marken K, Meinesz M, Miao H and Schwartz J 2004 The generation of 25.05 T using a 5.11 T $Bi_2Sr_2CaCu_2O_x$ superconducting insert coil *Supercond. Sci. Technol.* **17** 636–44

[7] Mbaruku A L and Schwartz J 2007 Statistical analysis of the electromechanical behavior of AgMg sheathed $Bi_2Sr_2CaCu_2O_{8+x}$ superconducting tapes using Weibull distributions *J. App. Phys.* **101** 073913

[8] Romanovskii V R and Watanabe K 2005 Nonlinear approximation for limiting current-carrying capacity of Ag-sheathed Bi2Sr2CaCu2O8 conductors *Supercond. Sci. Technol.* **18** 407–16

[9] Romanovskii V R, Watanabe K, Awaji S and Nishijima G 2006 Current-carrying capacity dependence of composite Bi2Sr2CaCu2O8 superconductors on the liquid coolant conditions *Supercond. Sci. Technol.* **19** 703–10

[10] Mbaruku A L, Marken K R, Meinesz M, Miao M, Sastry P V P S S and Schwartz J 2003 Effect of processing defects on stress–strain-I_c for AgMg Sheathed Bi-2212 tapes *IEEE Trans. Appl. Supercond.* **13** 1396–9